Measurements of production polarization and decay asymmetry for Ξ^- hyperons

R. Rameika,* A. Beretvas, L. Deck,† T. Devlin, K. B. Luk,‡ and R. Whitman§
Physics Department, Rutgers—The State University, Piscataway, New Jersey 08854

P. T. Cox,** E. C. Dukes,†† J. Dworkin,‡‡ and O. E. Overseth
Department of Physics, University of Michigan, Ann Arbor, Michigan 48109

R. Handler, B. Lundberg,§§ L. Pondrom, M. Sheaff, and C. Wilkinson
Physics Department, University of Wisconsin, Madison, Wisconsin 53706

K. Heller
Physics Department, The University of Minnesota, Minneapolis, Minnesota 55455
(Received 21 October 1985)

The polarization of Ξ^- hyperons produced by 400-GeV protons in the reaction $p + \mathrm{Be} \rightarrow \Xi^- + X$ has been measured as a function of momentum at two production angles. The average polarization for the full sample (192 110 events) was -0.108 ± 0.007. Comparisons are made with polarization measurements for other hyperons produced under similar conditions. From the same data, $\alpha_\Lambda \alpha_\Xi$ was measured to be $-0.303 \pm 0.004 \pm 0.004$, where α_Λ is the asymmetry parameter in the decay $\Lambda \rightarrow p\pi^-$, α_Ξ is the asymmetry parameter in the decay $\Xi^- \rightarrow \Lambda\pi^-$, and the uncertainties are statistical and systematic, respectively. This yields $\alpha_\Xi = -0.472 \pm 0.006 \pm 0.011$, where the systematic uncertainty is dominated by the uncertainty in α_Λ. An updated test of the $\Delta I = \frac{1}{2}$ rule in Ξ decay is presented.

I. INTRODUCTION

Polarization in reactions of the type

$$p + \text{nucleus} \rightarrow \text{hyperon} + \text{anything},$$

first observed for Λ production,[1] has since been found to be a general feature of hyperon production[2–4] over a wide range of incident proton energies.[5–10] The phenomenon is also observed when the target nucleus is a proton,[11,12] and for incident meson beams.[13–15] The first measurements of Ξ^- polarization in the reaction

$$p + \mathrm{Be} \rightarrow \Xi^- + X$$

are reported here. A comparison of these data with polarization measurements for other hyperons is presented.

With the same data sample, using a similar analysis technique, we have measured the asymmetry parameter in the decay $\Xi^- \rightarrow \Lambda\pi^-$. We present an updated computation of the $\Delta I = \frac{1}{2}$ test for the asymmetry parameters in Ξ^0 and Ξ^- decay.

II. APPARATUS AND PROCEDURES

The experiment was performed at Fermilab in the M2 diffracted proton beam. The experimental setup is shown in Fig. 1. The apparatus and techniques have been described extensively in other papers.[1–4,8–11,16] We present here only a general description of the setup and such features as are unique to this measurement. A much more extensive discussion is available in Ref. 17.

The 400-GeV proton beam was transported to a $\frac{1}{2}$-

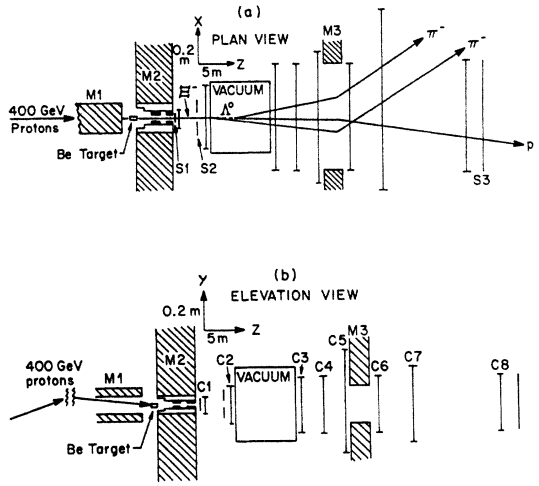

FIG. 1. (a) Plane and (b) elevation views of the charged-hyperon experimental apparatus. Note that the longitudinal and transverse distance scales are different. M_1 was the final dipole magnet in the beam transport system which brought the 400-GeV/c proton beam to the Be production target. The setting of M_1 controlled the angle in the vertical plane at which the beam struck the target. The 10-mrad bending angle of the hyperon beam in M_2 is not shown. S_1–S_3 were scintillation counters used in the trigger. C_1–C_8 were multiwire proportional chambers used to track the incident Ξ^- and the charged particles in its decay sequence. M_3 was a spectrometer magnet used to determine the momenta of the charged decay products. An example of an event is shown in the plan view. Some of the chambers were also used in the trigger (see text).

interaction-length, 6-mm-diam beryllium target where the Ξ^- were produced. The coordinate system at the production target was defined with $\hat{z}$ downstream along the centroid of the hyperon-beam channel, $\hat{y}$ vertically upward, and $\hat{x}$ completed a right-handed system.

The magnetic beam transport system allowed control of the angle at which the proton beam struck the target. Incident angles of ± 7.5 and ± 5.0 mrad in the y-z plane were obtained using a series of dipole magnets M_1. At the production target, the direction of the incident proton beam $\hat{k}_{in}$ and outgoing hyperon beam $\hat{k}_{out}$ defined the production plane, with the normal

$$\hat{n}=\hat{k}_{in}\times\hat{k}_{out}/|\hat{k}_{in}\times\hat{k}_{out}| \ . \tag{2.1}$$

The production angle was defined as positive when $\hat{n}$ pointed along $+\hat{x}$. It could be varied through both positive and negative values by changing the incident angle of the proton beam.

The trajectory of the hyperon beam was defined by the production target and by two tungsten collimators at the midpoint and exit of a 5.3-m-long magnet M_2. M_2 was operated with its field along $+\hat{y}$ to produce field integrals of 6.60 and 5.13 T m. The central ray through collimators had a 10-mrad bend angle in the x-z plane, corresponding to a 200-GeV/c negatively charged particle at the 6.6-T m setting. The actual mean momentum of the Ξ^- beam was about 10 GeV/c lower because the hyperon production spectrum decreased rapidly with momentum (Fig. 2). Data were also taken at 5.13 T m corresponding to a central channel momentum of 155 GeV/c. M_2 also provided a precession field for a measurement of the Ξ^- magnetic moment.[16]

The coordinate axes used for the detection system downstream of M_2 were rotated by 10 mrad with respect to the target coordinate system described above so that $\hat{z}$ was along the beam channel centroid at its exit, $\hat{y}$ vertical, and $\hat{x}$ horizontal as shown in Fig. 1.

The decay sequence observed in this experiment was

$$\Xi^-\rightarrow\Lambda\pi^- \ ,$$

$$\Lambda\rightarrow p\pi^- \ .$$

Because the baryon carries off most of the momentum at each stage of the decay chain, such an event has the distinctive feature of a high-momentum positively charged particle emerging from a negatively charged beam.

The charged particles of the decay sequence were detected in a spectrometer which consisted of multiwire proportional chambers (MWPC's C_1–C_8) and a superconducting analyzing magnet M_3, which had a transverse bending power of 0.95 GeV/c also in the x-z plane. The M_3 magnet had a 60-cm-horizontal, 20-cm-vertical aperture, and was 2 m long. The overall length of the spectrometer was 40 m. Scintillation counters S_1–S_3 were used in conjunction with fast signals from the chambers to trigger the data acquisition electronics. Signals from the left-half of C_7 and the right-half of C_8 were used to detect the coincidence of a negative (n) and positive (p) particle downstream of M_3. S_1 was a 10-cm-diam counter at the exit of M_2. S_2 was a 10×30-cm^2 counter with a 3.8×5-cm^2 central aperture used as a veto counter for the halo of the charged beam. S_3 was a 20×60-cm^2 counter which covered the active area of C_8, and was used as a timing signal for the fast electrons. The Ξ^- trigger required the coincidence

$$\Xi=S_1\cdot\bar{S}_2\cdot C_3\cdot C_7(n)\cdot C_8(p)\cdot S_3 \ . \tag{2.2}$$

Typical operating conditions yielded between 100 and 200 triggers during a 1-sec beam spill at an incident beam of 2×10^8 protons. A data tape consisting of approximately 80 000 triggers was produced in 2–3 hours. The production angle was reversed after every pair of tapes to provide roughly equal data samples at both positive and negative production angles taken under similar operating conditions. A total of 79 data tapes were written in approximately 200 hours of data taking.

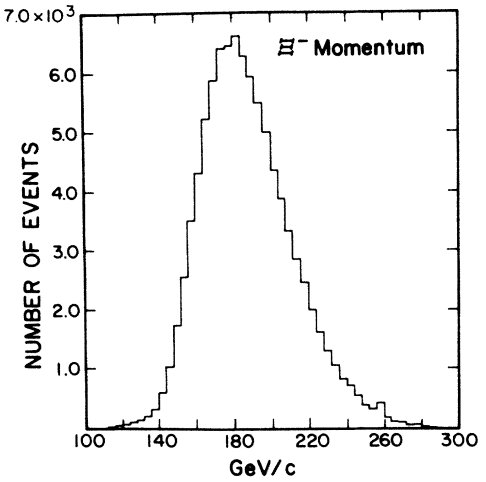

FIG. 2. The momentum distribution of reconstructed Ξ^- at 5.0 mrad production angle for an M_2 magnetic-field setting of 6.6 T m. The cutoff at low momenta was caused by the geometric acceptance of the beam channel. The high-momentum falloff is characteristic of the Ξ^- production cross section.

III. EVENT RECONSTRUCTION

Events were reconstructed from the MWPC data using a pattern-recognition, track-finding routine which searched for events having a three-track, two-vertex topology with $\chi^2<80$ (typically 20 DF). Both vertices were required to be upstream of C_3. Data from C_1 and C_2 were used in reconstruction of daughter particle trajectories where appropriate. One of the tracks was required to be a high-momentum, positively charged track, while the other two were of lower momentum and negatively charged. The momentum and charge were determined from the bend angle in M_3. Using the reconstructed slopes for the positive track and one of the negative tracks, a preliminary Λ vertex and direction were calculated. The intersection of this direction and the other negative track was labeled as the Ξ^- vertex. If the Λ vertex was found upstream of the Ξ^- vertex the negative tracks were interchanged and the vertices recalculated.

The yield of reconstructed three-track events was ap-

proximately 6% of the Ξ^- triggers. More than 50% of the triggers which failed to reconstruct as three-track events were single tracks, either pions—the major component of the negative beam—or Σ^-'s and their decay π^-'s, in coincidence with accidental hits which satisfied the trigger logic. Between 10% and 15% of the triggers were three-track events in which one of the negative tracks did not get through the analyzing magnet, or the decay(s) occurred too far downstream for the event to be reconstructed. The remainder of the raw triggers were multiparticle interactions which produced unrecognizable patterns in the chambers.

The kinematic fit to the hypothesis, $\Lambda \to p\pi^-$, was required to yield $\chi_\Lambda^2 < 20$. The Ξ^- invariant mass, formed from the fitted Λ and second π^-, was required to be between 1.306 and 1.338 GeV/c^2. The Λ and Ξ^- invariant-mass distributions are shown in Fig. 3.

In addition to the kinematic requirements, the Ξ^- momentum vector was projected back to the production target and required to be within a radius of 6.6 mm of the center of the target. The Ξ^- decay vertex was required to be downstream of the M_2 magnet. These requirements ensured that the Ξ^- had passed through the full length of the M_2 magnet.

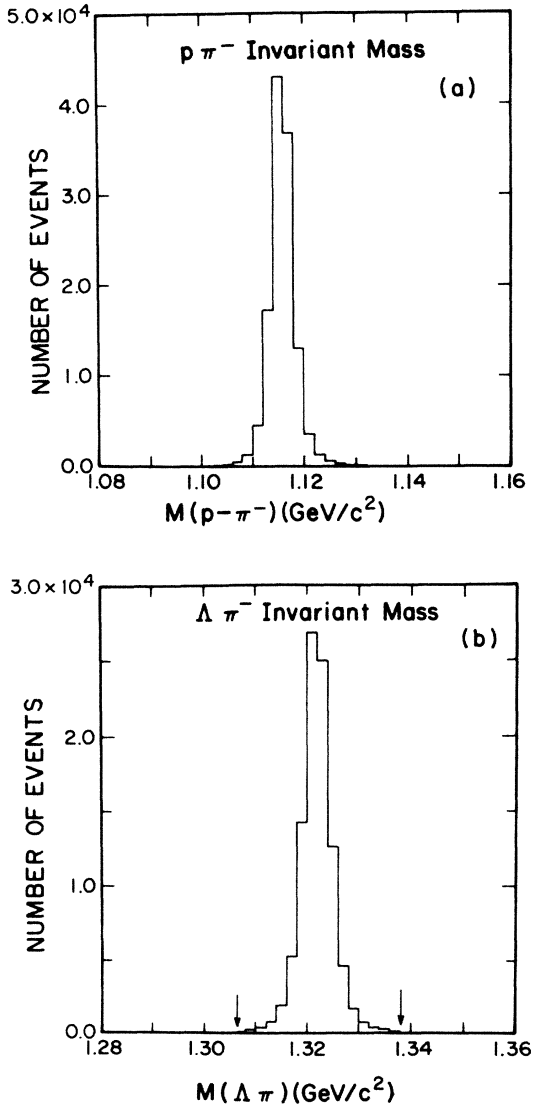

FIG. 3. Invariant-mass distributions for (a) $p\pi^-$ and (b) $\Lambda\pi^-$ selected as described in the text. The full widths at half maxima of the distributions are 5 and 7.5 MeV/c^2, respectively.

A total of 24% of all the reconstructed three-track events were eliminated by these requirements. Nine percent of these failures were Ξ^-'s which were incorrectly reconstructed (tracks or track segments misidentified) and so had an improper momentum determination. Fourteen percent were Ξ^-'s which were produced or decayed in the beam channel, and about 0.6% of the events were Ω^-'s. Over 218 000 Ξ^- events passed all selection criteria. It was estimated that there was less than a 1% background in the final sample. Details of event reconstruction and selection are given elsewhere.[17]

IV. ASYMMETRY ANALYSIS

Daughter Λ's from Ξ^- decay are polarized according to the expression[18]

$$\mathbf{P}_\Lambda = \frac{(\alpha_\Xi + \hat{\mathbf{\Lambda}}\cdot\mathbf{P}_\Xi)\hat{\mathbf{\Lambda}} - \beta_\Xi(\hat{\mathbf{\Lambda}}\times\mathbf{P}_\Xi) - \gamma_\Xi\hat{\mathbf{\Lambda}}\times(\hat{\mathbf{\Lambda}}\times\mathbf{P}_\Xi)}{1+\alpha_\Xi\hat{\mathbf{\Lambda}}\cdot\mathbf{P}_\Xi}\ , \tag{4.1}$$

where $\hat{\mathbf{\Lambda}}$ is the unit vector along the Λ momentum in the Ξ^- rest frame, and α_Ξ, β_Ξ, and γ_Ξ are the Ξ^- decay parameters which satisfy the relation $\alpha_\Xi^2+\beta_\Xi^2+\gamma_\Xi^2=1$. Assuming time-reversal invariance and no final-state interactions, $\beta_\Xi=0$, and the Λ polarization can be expressed

$$\mathbf{P}_\Lambda = \frac{\alpha_\Xi\hat{\mathbf{\Lambda}} + [(1-\gamma_\Xi)(\hat{\mathbf{\Lambda}}\cdot\mathbf{P}_\Xi)]\hat{\mathbf{\Lambda}} + \gamma_\Xi\mathbf{P}_\Xi}{1+\alpha_\Xi\hat{\mathbf{\Lambda}}\cdot\mathbf{P}_\Xi}\ , \tag{4.2}$$

where, in the initial iteration of the analysis of the full data set, we assume $\alpha_\Xi = -0.47$ from a crude early estimate based on part of the data, and $\gamma_\Xi = +0.88$ consistent with α_Ξ and the known sign.[19] When averaged over the experimental acceptance the $\hat{\mathbf{\Lambda}}\cdot\mathbf{P}_\Xi$ terms are very small. This, along with the large value of γ_Ξ, reduces Eq. (4.2) to the approximate expression

$$\mathbf{P}_\Lambda = \alpha_\Xi\hat{\mathbf{\Lambda}} + \gamma_\Xi\mathbf{P}_\Xi\ . \tag{4.3}$$

The polarization of the Λ sample was determined from the asymmetry of the proton distribution in the Λ rest frame

$$dN/d(\cos\theta) = (1+\mathbf{A}\cdot\hat{\mathbf{p}})/2\ , \tag{4.4}$$

where, in the absence of experimental biases,

$$\mathbf{A} = \alpha_\Lambda\mathbf{P}_\Lambda\ , \tag{4.5}$$

$\alpha_\Lambda = +0.642\pm0.013$ (Ref. 19), $\hat{\mathbf{p}}$ is the unit vector along the proton momentum in the Λ rest frame, and θ is the angle between $\hat{\mathbf{p}}$ and $\mathbf{A}$.

Since the direction of $\mathbf{P}_\Xi$ was not known at the outset, the asymmetries were determined with respect to each of the three directions $\hat{\mathbf{u}} = \hat{\mathbf{x}}, \hat{\mathbf{y}}, \hat{\mathbf{z}}$ (Ref. 20) from expressions similar to Eq. (4.4):

$$dN_u/d(\cos\theta_u) = (1+\mathbf{A}\cdot\hat{\mathbf{u}})/2\ , \tag{4.6}$$

where θ_u is the angle between $\mathbf{A}$ and $\hat{\mathbf{u}}$.

The evaluation of $\mathbf{P}_\Xi$ from these three distributions is best understood in terms of the approximation Eq. (4.3). For each event, the contribution of $\alpha_\Xi\hat{\mathbf{\Lambda}}$ to $\mathbf{P}_\Lambda$ was known. Further, the distribution of $\hat{\mathbf{\Lambda}}$ is random with respect to each of the fixed coordinates $\hat{\mathbf{u}}$, so that its contribution tends to vanish when averaged over the distribution. On the other hand, the direction of $\mathbf{P}_\Xi$ is fixed with respect to $\hat{\mathbf{u}}$, so that the determination of the asymmetries from Eq. (4.5) gives, to a good approximation,

$$\mathbf{A}=\alpha_\Lambda\mathbf{P}_\Lambda=\alpha_\Lambda\gamma_\Xi\mathbf{P}_\Xi \ . \tag{4.7}$$

In practice, the exact expression, Eq. (4.2), was used, but the results did not differ from those using Eq. (4.3).

Once $\mathbf{P}_\Xi$ was determined, it was then possible to reanalyze the data to obtain a more precise determination of the product, $\alpha_\Lambda\alpha_\Xi$. This was done by setting $\hat{\mathbf{u}}=\hat{\mathbf{\Lambda}}$ in Eq. (4.6). In this case, the $\alpha_\Xi\hat{\mathbf{\Lambda}}$ term in Eq. (4.3) is emphasized, and the other term, $\gamma_\Xi\mathbf{P}_\Xi$, tends to vanish when averaged over all possible directions of $\hat{\mathbf{\Lambda}}$. Any effects due to $\mathbf{P}_\Xi$ are further eliminated when the data samples for positive and negative production angles are combined. In the combined sample $\mathbf{P}_\Xi<10^{-3}$, i.e., zero to a good approximation. A second iteration of the two procedures produces changes less than 0.3 standard deviations in the asymmetries.

The contribution of the experimental acceptance term to the proton distribution was included using a hybrid Monte Carlo technique in which the Monte Carlo events were derived from the real events.[20] This procedure as applied to Ξ^0 polarization, has been described elsewhere.[2,21,22]

V. CALCULATION OF THE POLARIZATION

The method above yielded a set of measured asymmetries along each of the coordinate axes for data taken at positive and negative values of the production angle for the three settings of production angle and precession field. This section describes the procedures used to eliminate some remaining small experimental biases and to yield $\mathbf{P}_\Xi$ downstream of M_2. The measurement of $\mathbf{P}_\Xi$ at two values of the precession field eliminates ambiguities in the precession angle in M_2, and allows a determination of the polarization vector at production.

Parity conservation in the strong-interaction production process requires that the spin of the produced hyperon be either parallel or antiparallel to the normal to the production plane, i.e., along the direction $\hat{\mathbf{n}}$ of Eq. (2.1). Reversing the production angle reverses $\hat{\mathbf{n}}$ and the direction of the initial polarization. This provides a powerful method for removing any remaining experimental biases not simulated by the hybrid Monte Carlo method.

We assume that the detection apparatus and software efficiency are not affected by the production angle reversal, and that asymmetries induced from these effects do not reverse.[23] Thus, the measured asymmetry along a spatial axis $\hat{\mathbf{u}}$ for Ξ^- produced at an angle $\pm\theta$ can be expressed

$$A_u(\pm)=\pm\alpha_\Lambda P_u+B_u \ , \tag{5.1}$$

where B_u represents the residual experimental bias. The biases can be determined and removed by calculating the sums and differences:

$$\alpha_\Lambda P_u=[A_u(+)-A_u(-)]/2 \ , \tag{5.2}$$

$$B_u=[A_u(+)+A_u(-)]/2 \ . \tag{5.3}$$

For this reason equal amounts of data were taken at both positive and negative production angles. The results from Eqs. (5.2) and (5.3) are presented in Table I.

Any polarization along $\hat{\mathbf{y}}$ would be parity violating, since it would be in the production plane, and the precession in M_2, entirely in the x-z plane, could not produce it. No such polarization was observed. The combined result from all data samples yields $\alpha_\Lambda P_{y\Lambda}=-0.0014\pm0.0034$. This yields a value for the parity-violating polarization at the production target of $P_{y\Xi}=-0.0024\pm0.0060$. In the subsequent discussion, it will be assumed that this component is zero.

The measured Ξ^- polarization in an experiment of this type is the polarization of the sample after the particle spins have precessed in the M_2 field. To determine the production polarization, one must correct for the precession. Ambiguities in determining the precession angle exist because it is not known *a priori* whether the polarization vector at the production target was along $+\hat{\mathbf{x}}$ or $-\hat{\mathbf{x}}$. Further, the precession can be clockwise or anticlockwise, and it can be determined only modulo 360°. These ambiguities can be resolved by measuring the polarization vector for two values of the precession field in M_2. This was discussed in detail in Refs. 16 and 17 which described the measurement of the Ξ^- magnetic moment from the same data.

For each value of the field in M_2, the precession angle was calculated with respect to $\hat{\mathbf{x}}$ using $\phi=\arctan(P_z/P_x)$, where P_z and P_x were the bias-free asymmetries. The angle obeys the precession equation:

$$\phi=(q/\beta mc^2)(g/2-1)\int B\,dl \ , \tag{5.4}$$

where $\beta\simeq0.999\,98$ and $q/\beta mc^2=-13.01$ for ϕ in degrees and $\int B\,dl$ in T m. The results[16] are consistent only with the initial polarization along $-\hat{\mathbf{x}}$, i.e., antiparallel to $\hat{\mathbf{k}}_{\text{in}}\times\hat{\mathbf{k}}_{\text{out}}$.

The polarization and biases were measured as functions of the momentum of the Ξ^- using a χ^2 fit which included all the data, binned by momentum p, for various production angles and precession fields. The χ^2 was minimized with respect to the magnitude of the polarization $P_0(p)$ and the biases along $\hat{\mathbf{x}}$ and $\hat{\mathbf{z}}$, $B_x(p)$ and $B_z(p)$. The precession angles ϕ for the two values of $\int B\,dl$ were required to agree with Eq. (5.4) with $(g/2-1)$ as a parameter of the fit. The expression for χ^2 is

$$\chi^2=\sum_{ijk}\left\{\frac{[A_x(i,j,k)-B_x(i)\pm P_0(i,j)\cos\phi_j]^2}{\sigma_x^2(i,j,k)}+\frac{[A_z(i,j,k)-B_z(i)\pm P_0(i,j)\sin\phi_j]^2}{\sigma_z^2(i,j,k)}\right\} , \tag{5.5}$$

TABLE I. Momentum-averaged asymmetries, biases, and polarizations. The $A_u(\pm)$ are the measured asymmetries along each of the coordinate axes, $\hat{u}=\hat{x},\hat{y},\hat{z}$, for positive (+) and negative (−) production angles. The quantities $\alpha_\Lambda P_{u\Lambda}$ are the "physics" asymmetries determined from Eq. (5.2), and B_u are the instrumental asymmetries determined from Eq. (5.3).

	5 mr, 6.60 Tm	5 mr, 5.13 Tm	7.5 mr, 5.13 Tm
$A_x(+)$	−0.046±0.007	−0.027±0.012	−0.043±0.014
$A_x(-)$	+0.074±0.007	+0.066±0.012	+0.082±0.014
$A_y(+)$	−0.006±0.006	−0.035±0.012	+0.004±0.014
$A_y(-)$	−0.003±0.006	−0.031±0.012	−0.006±0.014
$A_z(+)$	+0.035±0.007	+0.019±0.013	−0.010±0.017
$A_z(-)$	+0.048±0.007	+0.018±0.014	−0.030±0.016
$\alpha_\Lambda P_{x\Lambda}$	−0.060±0.005	−0.046±0.008	−0.062±0.010
$\alpha_\Lambda P_{y\Lambda}$	−0.002±0.004	−0.003±0.008	+0.005±0.010
$\alpha_\Lambda P_{z\Lambda}$	−0.005±0.005	+0.001±0.010	+0.010±0.012
B_x	+0.012±0.005	+0.018±0.008	+0.019±0.010
B_y	−0.004±0.004	−0.033±0.008	−0.001±0.010
B_z	+0.041±0.005	+0.019±0.010	−0.021±0.012

where i, j, and k are the indices of the momentum bin, the field integral, and the production angle, respectively. The upper sign in Eq. (5.5) is taken for positive production angles and the lower sign for negative production angles. $A_x(i,j,k)$, $A_z(i,j,k)$, $\sigma_x(i,j,k)$, and $\sigma_z(i,j,k)$ are the measured asymmetries and uncertainties. The results of this global fit to all the data are given in Table II.

The biases, which were substantial only in the z asymmetry at high momentum, were determined to be the result of a loss of events by the reconstruction program. The major cause of this loss was the narrow opening angles between the particles at high momentum which led to track misidentification, and hence elimination from the sample. Biases of the same magnitude and momentum dependence were also found when a sample of "external" Monte Carlo events[24] was treated in the same manner as the real data.

To ensure that the results were not affected by various cuts imposed on the sample of Ξ^- included in the analysis, these cuts were varied in a number of ways and the effect on the polarization was studied. While there were significant changes in the biases, the changes in the polarization signal never exceeded 0.6 standard deviations.

A comparison of the Ξ^- polarization and that measured for other hyperons, Λ, Ξ^0, Σ^-, and Σ^+, shows that the direction of polarization at production is the same as in the neutral hyperons,[2,5–9] and opposite that of Σ^+ and Σ^- (Refs. 3 and 4). The magnitude of the Ξ^- polarization at 5 mrad tends to be smaller in magnitude than that observed for the neutral hyperons, though at 7.5 mrad any difference is not obvious. The Ξ^- polarization exhibits a similar dependence on the kinematic variables, Feynman x (x_F) and transverse momentum (p_T). The Ξ^- polarization is compared with the inclusive polarization of the neutral hyperons in Fig. 4.

The discovery of inclusive polarization in the Ξ^- hyperon supports the evidence that all inclusively produced hyperons are polarized. A number of simple quark-model pictures of hadron production predict some of the features observed in inclusive polarization.[25,26]

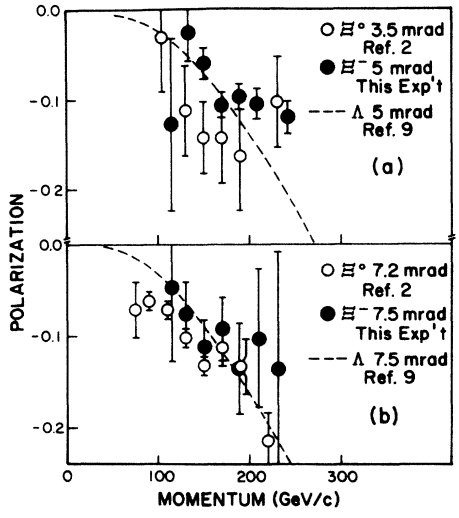

FIG. 4. The Ξ^- polarization is shown as a function of momentum for (a) 5 and (b) 7.5 mrad production angle. For comparison, the polarizations of Ξ^0 and Λ produced under roughly similar conditions are also shown. The Λ polarization is from a fit to several precise experiments (Ref. 9). Note that the Ξ^0 polarization in (a) is at 3.5 mrad. The sign convention is defined so that positive polarization is along the direction $\hat{k}_{in}\times\hat{k}_{out}$, where $\hat{k}_{in}$ and $\hat{k}_{out}$ are the directions of the incoming proton and outgoing hyperon, respectively.

TABLE II. Results of a global fit to the polarization data. The parameters of the global fit to the asymmetries from the several data sets were the polarization as a function of momentum and production angle, the biases as functions of momentum, and $(g/2-1)$ which governs the precession of the polarization vector in M_2. Reference 16 reported the fitted value, $(g/2-1)=-0.03\pm0.05$. The value of χ^2 was 27 for 27 degrees of freedom.

Momentum (GeV/c)	p_T (GeV/c)	x_F	P_0 (5 mrad)
115	0.58	0.29	-0.126 ± 0.095
133	0.67	0.33	-0.025 ± 0.031
151	0.76	0.38	-0.058 ± 0.017
170	0.85	0.43	-0.104 ± 0.014
189	0.95	0.48	-0.094 ± 0.014
209	1.05	0.52	-0.102 ± 0.017
242	1.21	0.61	-0.117 ± 0.018
Momentum (GeV/c)	**p_T (GeV/c)**	**x_F**	**P_0 (7.5 mrad)**
115	0.86	0.29	-0.046 ± 0.078
131	0.98	0.33	-0.074 ± 0.034
150	1.13	0.38	-0.110 ± 0.029
169	1.27	0.42	-0.090 ± 0.034
189	1.42	0.47	-0.133 ± 0.049
209	1.55	0.52	-0.099 ± 0.075
231	1.73	0.58	-0.133 ± 0.128
Momentum (GeV/c)	**B_x**		**B_z**
115	$+0.039\pm0.038$		-0.016 ± 0.059
133	$+0.020\pm0.014$		-0.036 ± 0.018
151	$+0.023\pm0.009$		$+0.003\pm0.010$
170	$+0.019\pm0.008$		$+0.017\pm0.009$
189	$+0.014\pm0.009$		$+0.026\pm0.009$
209	$+0.014\pm0.011$		$+0.059\pm0.012$
239	-0.004 ± 0.012		$+0.090\pm0.013$

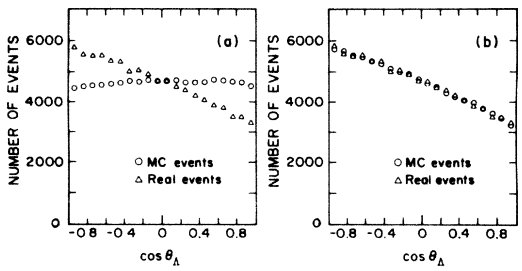

FIG. 5. Angular distributions of the proton in the decay of the daughter Λ in the Ξ^- decay sequence. The angle θ_Λ is measured between the vector $\hat{\Lambda}$ (defined in the text) and the direction of the proton, expressed in the Λ c.m. system. Both real data and events generated by a Monte Carlo (MC) calculation are shown. Uncertainties are smaller than the size of the symbols plotted. In (a) the distribution of MC events was generated under the assumption $\alpha_\Lambda\alpha_\Xi=0$. The resulting curve is an indication of the uniformity of the acceptance as a function of θ_Λ. In (b) the distribution of MC events was generated under the assumption $\alpha_\Lambda\alpha_\Xi=-0.303$. The χ^2 comparison of this MC distribution and the real data distribution yields 19.3 for 19 DF.

VI. ASYMMETRY IN THE DECAY $\Xi^-\to\Lambda\pi^-$

A. Results

A measurement of proton asymmetry for an unpolarized sample of Ξ^- with $\hat{u}=\hat{\Lambda}$ in Eq. (4.6) is a direct measure of the quantity $\alpha_\Lambda\alpha_\Xi$. Had the acceptance of the apparatus been perfect, the value of $\alpha_\Lambda\alpha_\Xi$ could have been measured directly from the slope of the $\cos\theta_\Lambda$ distribution. In order to correct for the lack of perfect acceptance, a sample of Monte Carlo events was generated with an asymmetry which was adjusted until the Monte Carlo distribution matched the data with minimum χ^2. Figure 5 compares these distributions for the real data, and for the Monte Carlo sample under the assumptions of zero asymmetry and the final fitted value: $\alpha_\Lambda\alpha_\Xi=-0.303\pm0.004$. The uncertainty is purely statistical, and the χ^2 for the fit was 19.3 for 19 degrees of freedom.

Since the asymmetry in this case cannot be reversed, no bias cancellation is possible. It can be argued that any bias is small. The acceptance of the apparatus is nearly constant over the full range of $\cos\theta_\Lambda$ as can be seen in Fig. 5. This is true because $\hat{\Lambda}$ is not constrained to any particular direction in space. Any failure of the Monte Carlo procedure to simulate the true acceptance affects all values of $\cos\theta_\Lambda$ approximately equally.

The result was tested for systematic errors in a manner similar to that employed for the polarization measurement. Cuts were varied and the full first- and second-level iteration repeated in each case. Data sets taken under different conditions of production angle, field integral, and trigger configuration were analyzed independently, and, in configurations where the number of events permitted, data in different Ξ^--momentum bins were analyzed separately. Details of these analyses are given in Ref. 17. The systematic differences observed were at the same level as the statistical uncertainty. Our final result, based on 192 110 events, is $\alpha_\Lambda\alpha_\Xi=-0.303\pm0.004\pm0.004$.

The accepted value of α_Λ [0.642 ± 0.013 (Ref. 19)] was used with this result to obtain the Ξ^- decay asymmetry:

$$\alpha_\Xi=-0.472\pm0.006\pm0.011\ , \tag{6.1}$$

where the systematic uncertainty is dominated by the uncertainty in α_Λ.

B. Comparison with other measurements

There is some disagreement between the high-statistics values of α_Ξ measured in recent hyperon-beam experiments -0.49 ± 0.04 (Ref. 27) and -0.462 ± 0.015 (Ref. 28), and earlier results from low-energy K^-p production of Ξ^- which have a weighted average of -0.385 ± 0.017. An ideogram for all these measurements is given by the

Particle Data Group (PDG).[19] Three new measurements of α_Ξ reinforce the disagreement: our result is in good agreement with the other hyperon-beam work, and two low-energy Ξ^- production experiments,[29,30] both of which yield values of -0.40 ± 0.03. This issue was discussed in Ref. 30 where the data are summarized in their Table VI. When our result is added, the average of the three hyperon-beam results (corrected, in the case of Ref. 28, for the current value of α_Λ) is $\alpha_\Xi=-0.470\pm0.010$. The average for the low-energy values as listed in the same table is $\alpha_\Xi=-0.391\pm0.013$. Both averages have $\chi^2<1.0$. If all six numbers are combined, the average is -0.443 ± 0.008 with $\chi^2/\mathrm{DF}=24/5$; $P(\chi^2)=0.0002$. The statistical significance of this is difficult to interpret, since one of the inputs is already an average of 11 older, mostly bubble-chamber experiments done prior to Ref. 27. If they are dropped, the average of the five most recent measurements becomes -0.458 ± 0.009 with $\chi^2/\mathrm{DF}=9.4/4$; $P(\chi^2)=0.05$.

C. Discussion

It is useful to pursue this discussion under the assumption, still debatable, that the difference between the hyperon-beam results and those from the other experiments is real. The aspects discussed in Ref. 30 will not be repeated here. That experiment and the present one have been reexamined for systematic errors and none has been found. We have paid particular attention to backgrounds. With the lowest possible cuts, which leave an unambiguous background of 20% in the Ξ^- sample, $\alpha_\Lambda\alpha_\Xi$ is -0.285. If some of this background remains in the final cut sample, removing it would only enhance the discrepancy. As the cuts are tightened in various orders, the value plateaus at our quoted result. With extremely tight cuts, the biases in the polarization measurement increase, although the polarization itself remains stable. Our final cuts fall in the plateau—low-bias region and leave a background of $<1\%$. In order for this background to explain the discrepancy, it would need an asymmetry of 4.6, an unphysical value, and highly inconsistent with the stability of our answer as cuts are varied.

We have also examined the correctness of our Lorentz transformations and the order in which they were done: laboratory to Ξ^- rest system to Λ rest system. Reference 30 is the same in this respect.

The experiment of Ref. 30 (and most other low-energy K^-p experiments) was done in a magnetic field where the daughter Λ precessed after the decay. This was not considered in the original asymmetry analysis. Well within statistical uncertainties, their result does not change when Λ precession is included.[31]

The two types of experiments differ in the analysis method. The hyperon beam results came purely from an analysis of the daughter Λ helicity, whereas the other experiments did a multiparameter fit which included the helicity and the angular distribution of the Λ in the Ξ^- rest frame with respect to the Ξ^- polarization. The hyperon-beam experiments measure directly the product $\alpha_\Lambda\alpha_\Xi$, whereas the other experiments have constraints on α_Ξ independent of α_Λ. An error in the accepted value of α_Λ might explain the difference. It might be instructive to use the value of $\alpha_\Lambda\alpha_\Xi$ measured directly by the hyperon beams as a constraint in the multiparameter analysis of the other experiments. In addition, the value of α_Λ could be allowed to vary in these analyses.

D. The $\Delta I=\frac{1}{2}$ rule

In the decay $\Xi\to\Lambda\pi$, the s-wave ($L=0$) and p-wave ($L=1$) amplitudes are composed of the isospin-changing parts $\Delta I=\frac{1}{2}$ and $\Delta I=\frac{3}{2}$. These amplitudes can be related to experimental observables such as lifetime and asymmetry parameters.[32]

If only $\Delta I=\frac{1}{2}$ transitions are allowed, then an evaluation of the decay asymmetries and decay rates (Γ), with phase-space corrections, yields

$$\alpha^0/\alpha^-=0.977\,, \tag{6.2}$$

$$\Gamma^0/\Gamma^-=0.484\,, \tag{6.3}$$

where the superscripts (0) and ($-$) refer to Ξ^0 and Ξ^-, respectively. Experimental evidence indicates that the $\Delta I=\frac{1}{2}$ amplitudes dominate in hyperon decay, though the extent of that dominance has not been precisely determined, and theoretical attempts to explain this have not been overwhelmingly successful.[33]

The recent precise determination, $\alpha_\Lambda\alpha^0=-0.260\pm0.006$, of Ref. 34 and the result presented here, $\alpha_\Lambda\alpha^-\equiv0.303\pm0.006$, yield a difference

$$\Delta\alpha=(\alpha^0/\alpha^-)-0.977=-0.119\pm0.026\,, \tag{6.4}$$

which is more than four standard deviations from the prediction of the $\Delta I=\frac{1}{2}$ rule. Only the statistical uncertainties have been used in calculating this result because α_Λ cancels in the ratio, and because the apparatus and analysis techniques used in obtaining the two results were nearly identical, and some classes of systematic error are likely to cancel.

A similar treatment can be applied to the ratio of decay rates. Since the contribution of minor decay modes is negligible in comparison with the uncertainties in the total decay rates, the total rates are the inverse of the lifetimes. Using the current world averages,[19] we obtain

$$\Delta\Gamma=(\Gamma^0/\Gamma^-)-0.484=0.081\pm0.020\,. \tag{6.5}$$

Again, the difference from the pure $\Delta I=\frac{1}{2}$ prediction is about four standard deviations.

If we assume the existence of a $\Delta I=\frac{3}{2}$ contribution in both the s-wave and p-wave amplitudes in the decay, then the differences above can be expressed in terms of the amplitude ratios[32]

$$\Delta\alpha=1.37(S_3/S_1-P_3/P_1)\,, \tag{6.6}$$

$$\Delta\Gamma=-1.44(S_3/S_1)-0.06(P_3/P_1)\,, \tag{6.7}$$

where the subscripts 1 and 3 refer to the $\Delta I=\frac{1}{2}$ and $\frac{3}{2}$ amplitudes, respectively. Solving this, we find

$$S_3/S_1=-0.057\pm0.013\,, \tag{6.8}$$

$$P_3/P_1=0.029\pm0.023\,. \tag{6.9}$$

An analysis similar to this one was presented in Ref. 10. Amplitude ratios of this same order have long been demonstrated in the study of K decay.[35,36]

ACKNOWLEDGMENTS

Reference 30 appeared after this manuscript was submitted for publication and raised questions which required a response on our part. We thank Dr. Brian Meadows for his prompt, enthusiastic cooperation in a reexamination of both experiments which allowed us to publish without undue delay. We gratefully acknowledge the help of the staff of Fermilab, in particular the Meson Laboratory during this experiment. This work was supported in part by the National Science Foundation and the Department of Energy.

---

*Present address: M.S. 122, Fermilab, P.O. Box 500, Batavia, IL 60510.

†Present address: Honeywell Corp., 10400 Yellow Circle Dr., Minnetonka, MI 55343.

‡Present address: M.S. 221, Fermilab, P.O. Box 500, Batavia, IL 60510.

§Present address: The Machlett Laboratories, Inc., 1063 Hope St., Stamford, CT 06907.

**Present address: Physics Department, Rockefeller University, New York, NY 10021; Mailing address: EP Division, CERN, CH-1211, Geneva 23, Switzerland.

††Present address: EP Division, CERN, CH-1211, Geneva 23, Switzerland.

‡‡Present address: Fonar Corporation, 110 Marcus Dr., Melville, NY 11747.

§§Present address: Physics Department, Ohio State University, Columbus, OH 43210; Mailing address: M.S. 221, Fermilab, P.O. Box 500, Batavia, IL 60510.

[1]G. Bunce *et al.*, Phys. Rev. Lett. **36**, 1113 (1976).

[2]p + nucleus$\rightarrow\Xi^0+X$ at 400 GeV, K. Heller *et al.*, Phys. Rev. Lett. **51**, 2025 (1983).

[3]p + nucleus$\rightarrow\Sigma^+ +X$ at 400 GeV, C. Wilkinson *et al.*, Phys. Rev. Lett. **46**, 803 (1981); C. Ankenbrandt *et al.*, *ibid.* **51**, 863 (1983).

[4]p + nucleus$\rightarrow\Sigma^- +X$ at 400 GeV, L. Deck *et al.*, Phys. Rev. D **38**, 1 (1983); Y. Y. Wah *et al.*, Phys. Rev. Lett. **55**, 2551 (1985).

[5]p + nucleus$\rightarrow\Lambda+X$ at 12 GeV, F. Abe *et al.*, Phys. Rev. Lett. **50**, 1102 (1983).

[6]p + nucleus$\rightarrow\Lambda+X$ at 24 GeV, K. Heller *et al.*, Phys. Lett. **68B**, 480 (1977).

[7]p + nucleus$\rightarrow\Lambda+X$ at 28 GeV, F. Lomanno *et al.*, Phys. Rev. Lett. **43**, 1905 (1979).

[8]p + nucleus$\rightarrow\Lambda+X$ at 300 GeV, P. Skubic *et al.*, Phys. Rev. D **18**, 3115 (1978).

[9]p + nucleus$\rightarrow\Lambda+X$ at 400 GeV, K. Heller *et al.*, Phys. Rev. Lett. **41**, 607 (1978); **45**, 1043(E) (1980); B. Lundberg, Ph.D. thesis, University of Wisconsin, 1984. The latter work contains a functional fit to all the available 400-GeV data.

[10]For a review of this and related subjects, see Lee G. Pondrom, Phys. Rep. **122**, 58 (1985).

[11]$p+p\rightarrow\Lambda+X$ at 400 GeV, R. Grobel *et al.* (unpublished); Ronald A. Grobel, Ph.D. thesis, University of Wisconsin, 1980. The data are reported in Ref. 10.

[12]$p+p\rightarrow\Lambda+X$ at 63-GeV center-of-mass energy, S. Erhan *et al.*, Phys. Lett. **82B**, 301 (1979).

[13]$\pi^-+p\rightarrow\Lambda+X$, J. Bensinger *et al.*, Phys. Rev. Lett. **50**, 313 (1983).

[14]$K^-+p\rightarrow\Lambda+X$, M. L. Faccini-Turleur *et al.*, Z. Phys. C **1**, 19 (1979).

[15]$K^++p\rightarrow\bar{\Lambda}+X$, I. V. Ajinenko *et al.*, Phys. Lett. **121B**, 183 (1983).

[16]R. Rameika *et al.*, Phys. Rev. Lett. **52**, 581 (1984).

[17]Regina A. Rameika, Ph.D. thesis, Rutgers University, 1981.

[18]T. D. Lee and C. N. Yang, Phys. Rev. **108**, 1645 (1957); G. Källen, *Elementary Particle Physics* (Addison-Wesley, Reading, Mass., 1964).

[19]Particle Data Group, Rev. Mod. Phys. **56**, S126 (1984).

[20]The coordinate axes, $\hat{\mathbf{x}}$, $\hat{\mathbf{y}}$, and $\hat{\mathbf{z}}$, were nearly parallel to the laboratory coordinate axes downstream of M_2 described in Sec. II. Small rotations from that system, of order 1 mrad, were made for each event to align $\hat{\mathbf{z}}$ with the laboratory Ξ^- momentum. This preserved the validity of the precession equation to be discussed in Sec. V.

[21]G. Bunce, Nucl. Instrum. Methods **172**, 553 (1980).

[22]P. T. Cox *et al.*, Phys. Rev. Lett. **46**, 877 (1981).

[23]The effects of changes in beam phase space have been studied carefully with data [L. Schachinger *et al.*, Phys. Rev. Lett. **41**, 1348 (1978); P. T. Cox *et al.*, *ibid.* **46**, 877 (1981); L. Deck *et al.* (Ref. 4); C. Wilkinson *et al.* (unpublished)] and with Monte Carlo simulations which reproduce observed effects. Changes in detector acceptance with production angle reversal occur whenever there exists a detector aperture or active volume only slightly larger than the beam-spot size at the longitudinal position of the spectrum. This is true even for detectors of daughter particles outside the primary hyperon beam. The present experiment has no such apertures, and Monte Carlo simulations indicate that its acceptance is particularly insensitive to production angle reversal.

[24]The "external" Monte Carlo events are not the same as the hybrid Monte Carlo events which were generated from each event processed through the asymmetry analysis as a built-in part of that analysis. See Refs. 17 and 20 for details.

[25]T. De Grand and H. Miettinen, Phys. Rev. D **24**, 2419 (1981).

[26]B. Andersson *et al.*, Phys. Lett. **85B**, 417 (1979).

[27]W. E. Cleland *et al.*, Phys. Rev. D **21**, 12 (1980).

[28]S. F. Biagi *et al.*, Phys. Lett. **112B**, 265 (1982).

[29]J. Bensinger *et al.*, Nucl. Phys. **B252**, 561 (1985).

[30]D. Aston *et al.*, Phys. Rev. D **32**, 2270 (1985).

[31]B. Meadows (private communication).

[32]O. E. Overseth and S. Pakvasa, Phys. Rev. **184**, 1663 (1969).

[33]J. Finjord and M. K. Gaillard, Phys. Rev. D **22**, 778 (1980).

[34]R. Handler *et al.*, Phys. Rev. D **25**, 639 (1982).

[35]T. Devlin and S. Barshay, Phys. Rev. Lett. **19**, 881 (1967).

[36]T. Devlin and J. Dickey, Rev. Mod. Phys. **51**, 237 (1979).